PRINT ISSN 1119-8362
Electronic ISSN 2659-1502

Full-text Available Online at
https://www.ajol.info/index.php/jasem
http://www.bioline.org.br/ja

J. Appl. Sci. Environ. Manage.
Vol. 27 (5) 979-984 May 2023

Prediction of Percentage Dilution in AISI 1020 Low Carbon Steel Welds Produced from Tungsten Inert Gas Welding

***[1]OHWOEKEVWO, JU; [1]OZIGAGUN, A; [1]ACHEBO, JI; [2]OBAHIAGBON, KO**

**[1]Department of Production Engineering, [2]Department of Chemical Engineering, University of Benin, Benin City, PMB. 1154, Nigeria*

**Corresponding Author Email: Jephtaruviefovwe@gmail.com*
Co-Authors Email: andrewzigs@yahoo.com; josephachebo@yahoo.co.uk; kobahiagbon@biu.edu.ng

ABSTRACT: The objective of this study is to predict the percentage dilution in AISI 1020 low carbon steel welds produced from tungsten inert gas welding using Artificial Neural Networking (ANN) approach. The regression plot showed R = 0.9992 as progress of training, R = 0.99865 as progress of validation and R = 0.85285 as progress of the training test. This led to overall correlation coefficient (R) of 0.90007 which signified that ANN is a robust tool for predicting the percentage of weld dilution. To test the reliability of the trained network, the ANN model was employed to predict its own value of percentage dilution using the same input parameters generated from the central composite design. Based on the observed and the predicted values of percentage dilution, a regression plot of outputs was thereafter generated, and r^2 value of 0.9876 was obtained which led to the conclusion that the trained network can be used to predict percentage dilution beyond the limit of experimentation. There was proximity in the results obtained, as both the experimental and predicted weld dilution fell between 44.5-71.55%. Hence, prediction adopted in this study can be applied in actual scenario without fear of inacuracies.

DOI: **https://dx.doi.org/10.4314/jasem.v27i5.14**

Cite this paper as: OHWOEKEVWO, J. U; OZIGAGUN, A; ACHEBO, J. I; OBAHIAGBON, K. O. (2023). Prediction of Percentage Dilution in AISI 1020 Low Carbon Steel Welds Produced from Tungsten Inert Gas Welding. *J. Appl. Sci. Environ. Manage.* 27 (5) 979-984

Dates: Received: 17 February 2023; Revised: 08 April 2023; Accepted: 16 April 2023
Published: 31 May 2023

Keywords: Prediction, Percentage dilution, Low carbon steel, Welding.

Welding technique involves the process of joining two or more pieces of metal together by the application of intense heat, pressure or both to melt the weld region of the metals in order to fuse permanently (Owunna and Ikpe, 2021). Considering Tungsten Inert Gas (TIG) welding which is the type of welding technique in this context, a non-consumable tungsten electrode is normally applied in the fusion of two or more metals through a localized application of heat and its dissipation through conduction into the parent metal to form a permanent joint. In addition, TIG welding also known as Gas Tungsten Arc Welding (GTAW) is a type of welding technique that is used for joining similar and dissimilar metals and their alloys (Ikpe et al., 2017; Owunna et al., 2018). In recent times, TIG welding techniques have been used in a number of studies conducted on weld dilution which is the change in composition of the weld metal due to mixing of the base metal or weld metal deposited previously. Shen et al. (2012) experimentally carried out series of measurements on specimens of submerged arc welded plates of ASTM A709 Grade 50 steel. The electrode melting efficiency increased initially and then decreased with increasing heat input but the plate melting efficiency and percentage dilution changed only slightly with it. Sun et al. (2019) investigated the thermal, metallurgical, and mechanical behavior of a three-pass groove weld formed by gas-tungsten arc welding in a 20 mm thick SA508 steel plate. Based on the projected cross -sectional areas for the fusion zone connected to each individual pass, the dilution for each pass was calculated as the proportion of base material in the weld metal. Thermocouple measurement results and cross-weld macrographs agreed with the

temperature forecasts. In cross-weld optical micrographs, the predicted and actual microstructures are qualitatively compared. The predictions for post-weld micro-constituents (such as the ferrite, bainite, and martensite fractions), based on a hardness microstructure correlation, are then quantitatively validated using the measured hardness. Moreover, Zhang (2021) used chemical composition analysis to compare the dilution values achieved using various methods, and the impact of heat inputs on weld dilution was investigated. The findings revealed that the mathematically proposed approach and the welding definition of dilution were in good agreement. The fact that a weld can be concentrated when the filler wire is rich in the same composition as the substrate was particularly observed when the weld dilution increased to a level higher than the critical value. Additionally, the technique showed that a bead's gross dilution is a combined result that is influenced by each distinct composition. Similarly, Lin (2020) in its experimental study affirmed that weld dilution is the change in chemical composition of the weld metal as a result of the base metal component that melts and begins to form the fusion zone. Its measurement is determined by the proportion of the base metal that contributes to the creation of the weld filet, and it varies depending on the type of join, pre-heat temperature, consumable, and welding parameters, among other condition. The performance of the welded materials depends on the solution in many applications; as a result, significant failures that occur may be attributed to this factor. Nweze and Achebo (2019) deployed TIG welding procedure to create a weld specimen, which was then entered into fuzzy logic program along with measurements of the percentage dilution. Voltage, current, gas flow rate, and welding speed were the process parameters. The collected results demonstrated that fuzzy logic tool is an effective predictor, and the model created was proven to be very effective in managing tasks of this nature, hence reducing the time, effort, and money lost in pre-welding operations. The present study is focused on the prediction of percentage dilution in AISI 1020 low carbon steel welds produced from tungsten inert gas welding using Artificial Neural Networking approach.

MATERIALS AND METHOD

AISI 1020 low carbon steel plate of 10 mm thickness each was cut into 60x40x10 mm (length x width x width) dimension. Emery paper (coarse: P24 grit size with 715 µm and fine: P80 grit size with 201 µm) was used to smoothen and eliminate rough particles and rust from the surface of specimen before welding the samples. This was followed by cleaning the surface of the samples to be welded with acetone in order to eliminate surface contamination. Using vertical milling machine, the welding samples (plates) were chamfered (2mm depth) with 45 degrees at the edge to form a V-groove angle while clamping it to a G-clamp. The Milling angle was done using a vertical milling machine. The welding was carried out with the plates properly clamped to avoid misalignment during welding process. TIG welding was applied to the chamfered area of the plate and filling the chaffered region using 2% thoriated tungsten electrode. This was achieved through the use of Dynasty 210 DX welding machine and 100 % Argon as the torch gas to protect the welding region from contaminants. Similar method was recently employed by Owunna et al., (2022) in a study on the application of SEM/EDS in fractographic investigation of TIG welded AISI 1020 fusion zones at distinct welding current steps. The TIG welding specifications employed in the welding process are presented in Table 1 while samples of the steel plates subjected to welding are shown in Fig 1.

Table 1. Materials and specifications used for the welding experimentation

S/N	Material Specification	Welding Specification
1	Welding Type	Tungsten Inert Gas (TIG)
2	Material	AISI 1020 Low Carbon Steel Plate
7	Material Thickness	10 mm
8	Filler Material	ER 70 S-6
9	Joint Type	Butt Joint (V-groove)
10	Joint Preparation	Abrasive Clean (Sand paper)/Acetone Wipe
11	Joint Gap	2 mm
12	Welding Current	D.C.E.N (Direct Current Electrode Negative)
13	Pulse Width	0.8 Seconds
14	Filler Rod Angle	15^o
15	Welding Torch Angle	45^o
16	Fixed Frequency	60Hz
17	Torch Type	Pro-torch (TIG Torch)
18	Tungsten Type	2% thoriated
19	Tungsten Size	3/1326" Diameter x 25.4 mm
20	Torch Gas	Argon (100%)
21	Heat Input Ratio	10.75 KJ/min
22	Weight of Filler Rod	78.5 Kg/m^2
23	Welding machine	Dynasty 210 DX
24	Clamp type	G-clamp for clamping the work pieces
25	Vertical milling machine	For milling the V-groove angle

K-type thermocouples were attached to the surface of the workpiece and the welding temperature was recorded at different points as the arc passed along the workpiece. Also, the welding torch passed over the plate at a height of 2.5mm from the workpiece at constant velocity of 1.72 m/s. The welding experiments were carried out according to the Central Composite Design Matrix (CCD) in Table 2 and in a random order to avoid any systematic error in the experiment. The welded samples are shown in Fig 1.

Table 2. Central composite design matrix (CCD)

std	Weld Runs	Block	Current	Voltage	Gas flow Rate
12	1	Block 1	250.23	23.5	13.5
16	2	Block 1	225	26	14.5
10	3	Block 1	250.23	24.5	14.5
19	4	Block 1	240	25	16
6	5	Block 1	225	25	16
13	6	Block 1	240	20.98	13.5
9	7	Block 1	199.77	24.5	13.5
18	8	Block 1	210	25	16
15	9	Block 1	199.77	26	11.98
14	10	Block 1	250.23	20.98	13.5
3	11	Block 1	240	22	11.98
11	12	Block 1	225	24.5	11.98
5	13	Block 1	210	22	16
7	14	Block 1	199.77	23.5	14.5
20	15	Block 1	210	20.98	14.5
8	16	Block 1	225	22	13.5
2	17	Block 1	199.77	26	11.98
17	18	Block 1	240	20.98	13
4	19	Block 1	210	22	16
1	20	Block 1	250.23	22	11.98

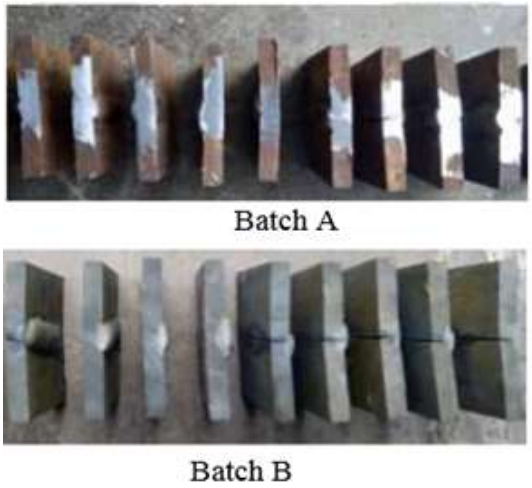

Fig. 1. Mild steel welded samples

The welded plates were checked for any visible defects and uniformity and then cross-examined at their axial midpoints to make test specimens. These 60 x 40 x10 mm dimensioned test specimens were polished and etched after completing all the experiments, samples were prepared for measurement of weld dilution by cutting, polishing and etching. For measuring the dilution, the samples were scanned on a scanner at 1:1 scale using optical microscope as shown in Fig 2. The bead geometry of these samples was measured by using Foxit reader software which was used in calculating the weld dilution by measuring penetration depth.

Modeling and Prediction Using Artificial Neural Network (ANN): To predict the response variables beyond the scope of experimentation, predictive model such as artificial neural network (ANN) was employed. To train a neural network for predicting the percentage diluton, a feed forward back propagation algorithm was used. The input layer of the network used the hyparbolic targent (tan-sigmoid) transfer function to calculate the layer output from the network input while the output layer used the linear (purelin) transfer function (Owunna and Ikpe, 2019). The number of hidden neuron was set at 10 neurons per layer and the network performance was monitored using the mean square error of regression (MSEREG). A learning rate of 0.01, momentum coefficient of 0.1, target error of 0.01, analysis update interval of 500 and a maximum training cycle of 1000 epochs was used.

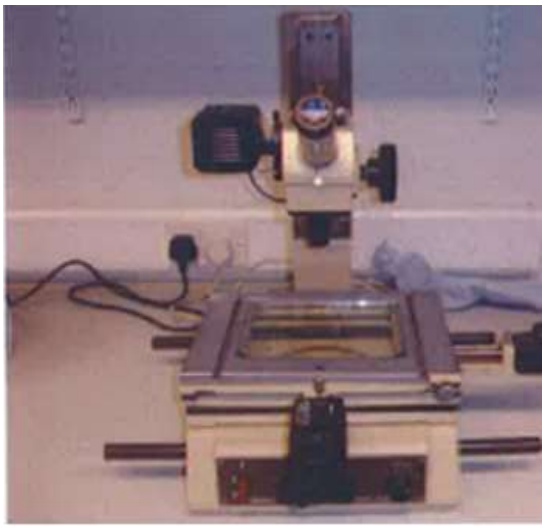

Fig. 2. Optical microscope

The network generation process divided the input data into training data sets, validation and testing. For this study, 60% of the data was employed to perform the network training, 25% for validating the network while the remaining 15% was used to test the performance of the network. Using these parameters, an optimum neural network architecture was generated as presented in Fig 3

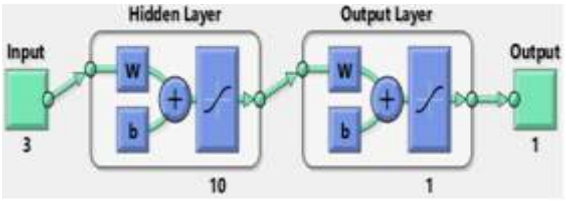

Fig. 3. Artificial neural network architecture for weld variable prediction

The same network architure was generated to predict the output response variables (weld dilutin) since the same input variables were used. The network properties for predicting weld variables upon which the designed architecture (see Fig 3) for the neural network is formed is shown in Fig 4. Figure 5 presents

the command button used for training the network. the input and targets are the factors and responses needed to predict, the output and errors are the results from the ANN trained prediction exercise. The network training diagram generated for the prediction of percentage dilution using back propagation neural network is presented in Fig 6.

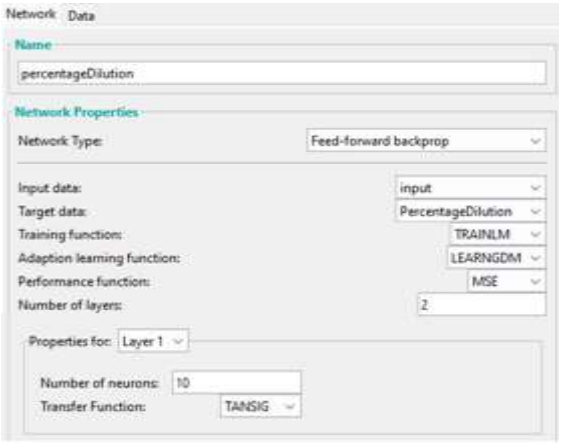

Fig. 4. Network properties for predicting weld variables

Fig. 5. ANN training/retraining environment for Percentage dilution

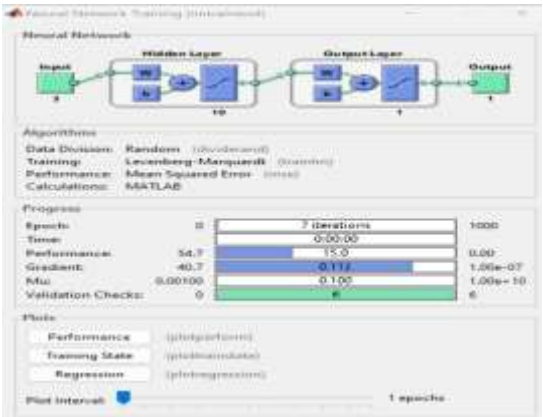

Fig. 6. Network training diagram for predicting percentage dilution

From the network training diagram of Fig. 7, it was observed that the maximum number of iteration needed for the network to reach its best performance was observed to be 7 iterations which is also lesser than the initial 1000 epochs. The gradient function was calculated to be 0.112 with a training gain (Mu) of 0.1. Validation check of six was recorded which is expected since the issue of wieght biased had been addressed via normalization of the raw data. A performance evaluation plot which shows the progress of training, validation and testing is presented in Fig 7.

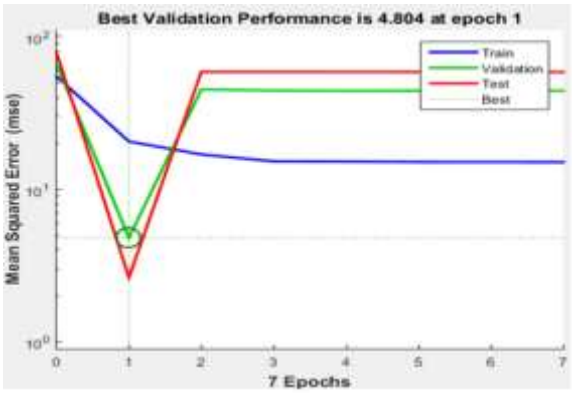

Fig. 7. Performance curve of trained network for predicting percentage dilution

From the performance plot of Fig 7, no evidence of over fitting was observed. In addition, similar trend was observed in the behavior of the training, validation and testing curve which is expected since the raw data were normalized before use. Lower mean square error is a fundamental criterion used to determine the training accuracy of a network.

RESULTS AND DISCUSSION

The training state, which shows the gradient function, the training gain (Mu) and the validation check, is presented in Fig 8. The regression plot which shows the correlation between the input variables (voltage, current and gas flow rate) and the target variable (percentage dilution) is presented in Fig 9.

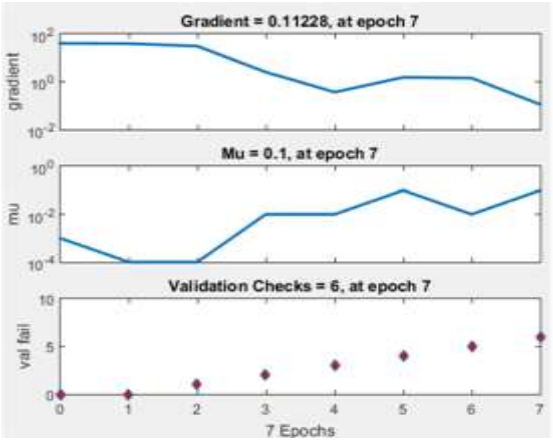

Fig. 8. Neural network training state

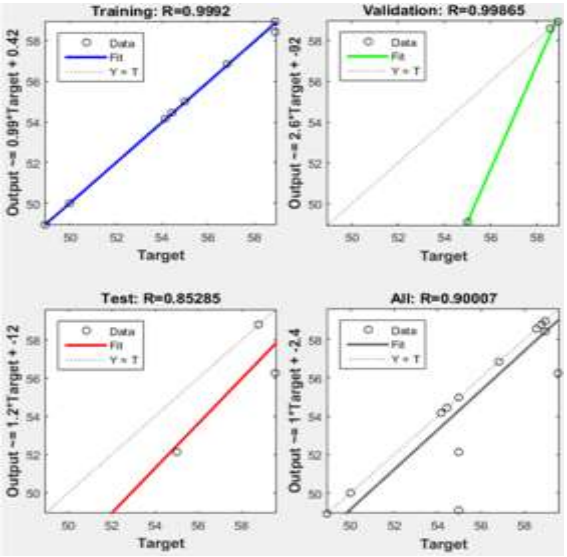

Fig. 9. Regression plot of input versus target variable for weld dilution

Figure 9 presents the training with correlation coefficient of 0.9992, validation with correlation coefficient of 0.99865 and testing with correlation coefficient of 0.85285 to give an overall correlation coefficient (R) of 0.90007 which signifies a robust prediction for the Percentage dilution. Based on the computed values of the correlation coefficient (R) as observed in Fig 9, it was observed that the network has been accurately trained and can be employed to predict the percentage of weld dilution beyond the scope of experimentation. To test the reliability of the trained network, the network was thereafter employed to predict its own values for percentage of weld dilution using the same set of input parameters (current, voltage and gas flow rate) generated from the central composite design. Based on the observed and the predicted values for percentage of weld dilution, a regression plot of outputs was thereafter generated as presented in Fig 10.

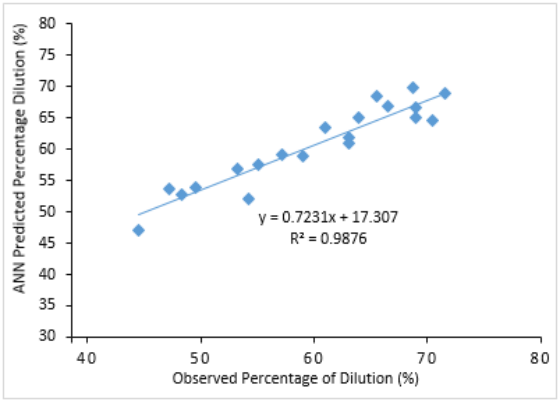

Fig. 10. Regression plot of observed versus predicted percentage dilution

Coefficient of determination (r^2) value of 0.9876 as observed in Fig 10 was obtained, indicating that the trained network can be used to predict the percentage of weld dilution beyond the limit of experimentation. Table 3 shows the ANN predicted percentage of weld dilution results compared with the experimental results. From Table 3, the experimental results and the ANN predicted results were compared side by side, and the plot presented in Fig 11 showed prediction accuracy of the network. Considering the graphical patterns in Fig 11, it is observed that both ANN predicted results and experimentally determined results correlated significantly with one another. For example, the maximum value experimentally obtained for weld dilution was 71.55% while the maximum value obtained using ANN approach was 69.83%.

Table 3: ANN predicted and experimentally determined results for percentage dilution

run	Current	Voltage	Gas flow rate	Exp percentage dilution	ANN percentage dilution
1	240	20.98	13.5	59.03	58.94
2	210	22	16	57.20	59.16
3	250.23	23.5	13.5	71.55	68.93
4	210	25	16	55.02	57.56
5	250.23	20.98	13.5	68.7	69.83
6	210	20.98	14.5	53.22	56.94
7	225	24.5	11.98	66.54	66.94
8	210	22	16	61.03	63.56
9	225	26.	14.5	68.94	66.56
10	225	25	16	63.12	61.78
11	199.77	23.5	14.5	63.04	60.94
12	210	22	16	54.23	52.18
13	250.23	24.5	14.5	69.02	65.03
14	199.77	26	11.98	47.2	53.56
15	250.23	22	11.98	70.46	64.56
16	225	22	13.5	48.36	52.8
17	199.77	26	11.98	44.5	47.04
18	240	25	16	65.55	68.56
19	240	20.98	13	63.94	65.1
20	199.77	24.5	13.5	49.54	53.99

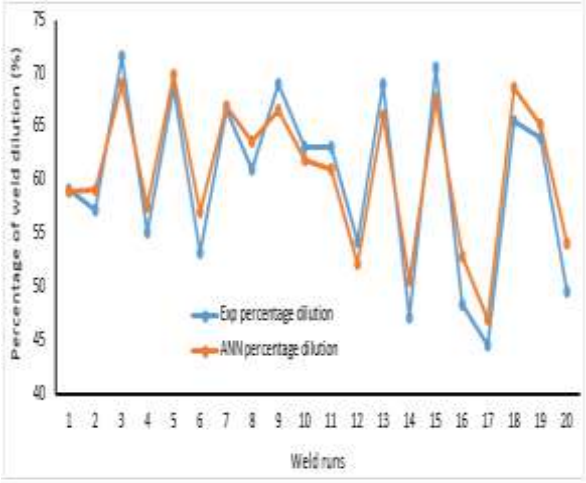

Fig. 11. Prediction accuracy of ANN in comparison to experimentally determined percentage dilution

Figure 12 represents a plot of welding current and weld dilution for different weld runs. It is observed from the Figure that the percentage of weld dilution for ANN and experimental results at each weld run increased as the welding current also increased and vice versa. This correlates with the findings of Kannan and Murugun (2006) which revealed that weld dilution increased as welding current also increase while welding speed decreased with increase in nozzle to plate distance and welding torch angle.

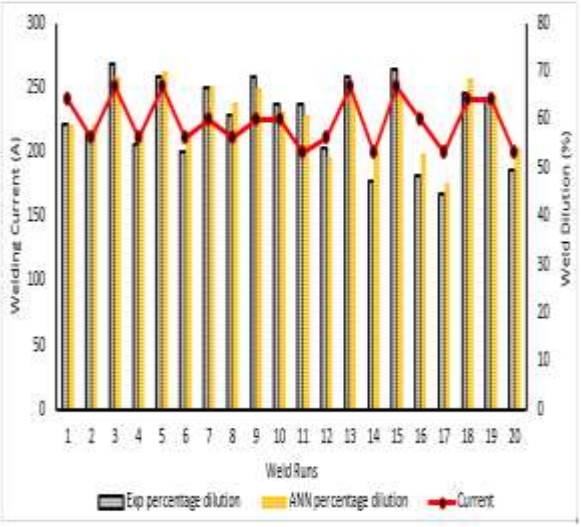

Fig. 12. Plot of welding current and weld dilution for different weld runs

*Conclusion***:** The findings in this study revealed that percentage of weld dilution for ANN and experimental results at each weld run increased as the welding current also increased and vice versa. The maximum and minimum values of weld dilution obtained through experimental and ANN approach were 71.55% and 69.83% as well as 44.5% and 47.04%, indicating that ANN is a robust computing tool that can be employed in the prediction of weld dilution percentages based on a predetermined input variables.

REFERENCE

Ikpe, AE; Owunna, I; Ememobong, I (2017). Effects of Arc Voltage and Welding Current on the Arc Length of Tungsten Inert Gas Welding (TIG), *Int J Eng Tech* 3(4): 213-221.

Kannan, T; Murugun, N (2006). Effect of flux cored arc welding process parameters on duplex stainless steel clad quality, *J mater Proc Tech* (176): 230-239.

Lin, Z; Ya, W; Subramanian, VV; Goulas, C; Castri, B; Hermans, MJ; Pathiraj, B (2020). Deposition of Stellite 6 alloy on steel substrates using wire and arc additive manufacturing, *The Int J Adv Manf Tech* 111: 411-426.

Nweze, S; Achebo, J (2019). The Use of Fuzzy Logic in Predicting Percentage (%) Dilution of Weld during TIG Welding Process, *Mater Sci App* 10: 406-422.

Owunna, I.; Ikpe, AE; Achebo, JI (2018). Temperature and Time Dependent Analysis of Tungsten Inert Gas Welding of Low Carbon Steel Plate Using Goldak Model Heat Source. *J. Appl. Sci. Environ. Manage.* 22(11): 1719-1725

Owunna, IB; Ikpe, AE (2019). Modelling and Prediction of the Mechanical Properties of TIG Welded Joint for AISI 4130 Low Carbon Steel Plates using Artificial Neural Network (ANN) Approach, *Nig J Tech* 38(1): 117-126.

Owunna, IB; Ikpe, AE (2021). Experimental and Numerical Optimization of Tungsten Inert Gas (TIG) Welding Process Parameters Relative to Mechanical Properties of AISI 1018 Mild Steel Plate, *Adv Eng Des Tech* 3: 132-145.

Owunna, IB; Ikpe, AE; Ohwoekevwo, JU (2022). Application of SEM/EDS in fractographic investigation of TIG welded AISI 1020 fusion zones at distinct welding current steps, *Arid Zone J Eng Tech Env* 18(2): 255-266.

Shen, S; Oguocha, IN; Yannacopoulos, S (2012). Effect of heat input on weld bead geometry of submerged arc welded ASTM A709 Grade 50 steel joints, *J Mater Proc Tech* 212(1): 286-294.

Sun, YL; Hamelin, CJ; Flint, TF; Vasileiou, AN; Francis, JA; Smith, MC (2019). Prediction of Dilution and Its Impact on the Metallurgical and Mechanical Behaviour of a Multipass Steel Weldment, *J Pres Vsl Tech* 141(6): 1-32.

Zhang, Z; Huang, X; Yao, P; Xue, J (2021). A New Method for Weld Dilution Calculation through Chemical Composition Analysis, *Met*, 11(131): 1-10.